CAAP Quarterly Report

Date of Report: January 10, 2015

Contract Number: DTPH56-14-S-N000006

Prepared for: Government Agency: DOT

Project Title: Laser peening for preventing pipe corrosion and failure

Prepared by: Board of Regent of the University of Nebraska for the University of Nebraska –Lincoln

Contact Information: Yonfeng Lu
Lott Distinguished Professor
Department of Electrical and Computer Engineering, University of Nebraska- Lincoln, 209N Walter Scott Engineering Center, Lincoln, NE 68588-0511
Phone: (402)472 8323
E-mail: ylu2@unl.edu

For quarterly period ending: December 31, 2014

Business and Activity Section

(a) Generated Commitments

There are no changes to the partners or cofounders that relate to work under CAAP award. During this reporting period, some equipment and supplies have been purchased, which are listed below.

Table 1. Equipment and supplies purchased

NOs.	**Instruments (supplies)**	**Manufacturer**	**Price ($)**
1	Galvano scanner	SCANLAB America, Inc.	14500.00
2	High-performance stage system	Aerotech, Inc	53850.00
3	Computer	Dell	919.98

4	Al-Mg alloy materials	Online metal	236.21
5	Stainless steel materials	Metal supermaket	245.00
6	Processing of metal materials	Lincoln machine	235.00

(b) Status Update of Past Quarter Activities

1. The major goal of the project

The ultimate goal of this project is to investigate and develop laser peening of pipeline steels to improve the corrosion resistance of stainless steel and carbon steel used for pipeline construction. The corrosion resistance of pipelines will be enhanced *via* the compressive residual stress created by laser-induced shock waves during laser peening. It is anticipated that by using laser shock peening in the construction of a pipeline, the reliability, safety, and lifespan of the nation's pipeline transportation system will be highly improved. As it has been stated in our proposal that the major goals of this project include four phase objectives. Table 2 summaries the current progress of each phase objective during this reporting period.

Table 2. The completion rate for each phase objective of the project

Phases	Major goals and milestones	Starting date (mm/dd/yy)	Ending date (mm/dd/yy)	Completion rate (%)
Phase 1	1) Experimental setup for laser cleaning developed	10/01/2014	12/31/2014	100
	2) Cleaning mechanism and parameter windows	01/01/2015	09/30/2016	0
	3) Real-time monitoring of cleaning process	01/01/2015	09/30/2016	0
Phase 2	1) A laser peening system developed	10/01/2014	12/31/2014	100
	2) Parameter windows for laser peening established	01/01/2015	09/30/2016	30
Phase 3	1) Surface morphology study of the laser-peened surfaces	01/01/2015	09/30/2016	30
	2) The residual stress of pipeline steels after laser cleaning and peening	01/01/2015	09/30/2016	0
	3) The corrosion resistance of laser-peened surface	01/01/2015	09/30/2016	0
Phase 4	Design a laser peening prototype system	06/30/2016	09/30/2016	0

The specific objectives during this reporting period

During this reporting period of the project (October 1, 2014 to December 31, 2014), the experimental setup for laser cleaning and laser shock peening (LSP) has been developed. The effects of LSP on the surface topography, nanoscale hardness, and elastic modulus of the samples manufactured by Mg-Al alloy and stainless steel, have been experimentally investigated and analyzed. The phased objectives and specific content are listed as follows:

(1) Developing the experimental setup for laser cleaning and laser shock peening;

(2) Preparation of the tested materials for laser shock peening;

(3) Optimization of processing parameters for laser shock peening;

(4) Surface morphology study of the laser-peened surfaces using optical microscopy and electrical scanning microscopy;

(5) Study of the surface nano-hardness and elastic modulus of the laser-peened stainless steel samples using nanoindentation technique.

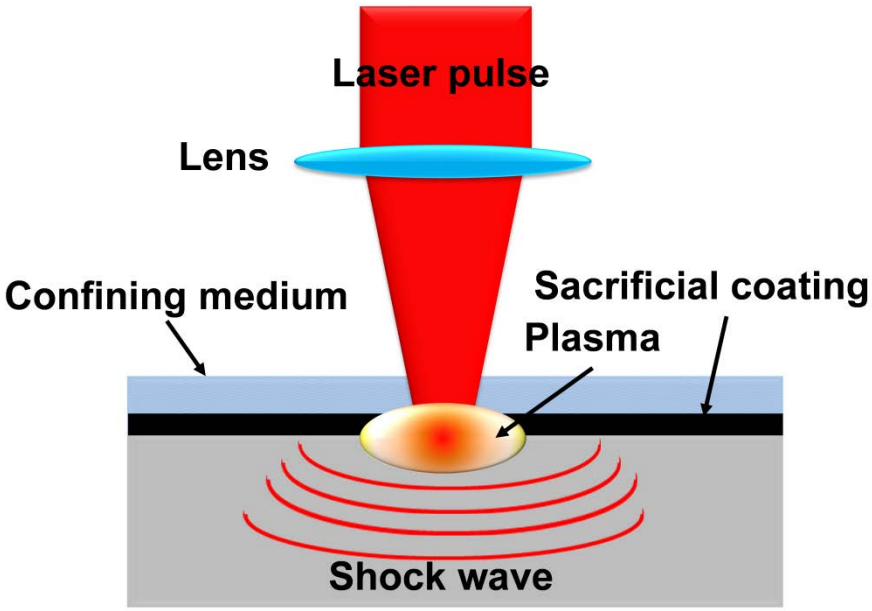

Fig. 1. Schematic of the principle of LSP.

2. Significant results

2.1 Experimental

2.1.1 Basic process

The basic process of LSP is illustrated in Fig. 1. LSP is a cold mechanical process where pressure waves caused by expanding plasma plastically deform the surface of a material. LSP uses a thin layer of ablative material that is opaque to the laser. The opaque ablative material,

typically black spray paint or tape, is used as a sacrificial layer in the early study by Fairland and Clauer [1]. The sacrificial layer also minimizes thermal effects on the surface caused by laser. The laser partially vaporizes the ablative layer to form high pressure plasma. The plasma, confined by a thin layer of water film (confining medium), expands rapidly resulting in a recoiling pressure wave on the order of GPa reported by Fariland et al. and Caslaru, et al. [2-3] The pressure wave is cold mechanical process that typically deforms the surface. The plasma-induced shock pressure causes severe plastic deformation, refined grain size, compressive residual stresses, and increased hardness at the surface and in the subsurface. As a result, the mechanical properties on the work-piece surface will be enhanced to improve the performance of corrosion and foreign objective damage.

Table 3. Chemical compositions of the tested materials (wt.%)

Material	C	Si	Mn	P	S	Ni	Cr	Mo	Fe
304 SS	0.06	0.41	0.90	0.032	0.001	8.47	19.07	---	Remainder
310 SS	0.25	0.75	2.0	0.045	0.030	20	25	0.75	Remainder
Material	**Mg**	**Si**	**Cr**	**Mn**	**Fe**				**Al**
5032 Al-Mg alloy	2.68	0.42	0.41	0.24	---				Remainder

Table 4. Mechanical properties of the tested materials

Material	Yield strength ($kgf\ mm^{-2}$)	Tensile strength ($kgf\ mm^{-2}$)	Elongation (%)	Specific gravity ($g\ cm^{-3}$)
304 SS	290	655	55 (50.8mm)	7.93
310 SS	205	515	40	7.75
5032 Al-Mg alloy	193	228	18	2.68

2.1.2 Material preparation

During this reporting period, the samples tested were prepared from 304 stainless steel (SS), 310 SS, and Al-Mg alloy plates. The tested samples of 304 SS, 310 SS, and Al-Mg alloy were cut into rectangular shape with dimensions of 30 mm × 30 mm (width × length) with different thickness of 2.3, 2, and 2 mm, respectively. The chemical compositions and mechanical properties of 304 SS, 310 SS, and 5032 Al-Mg alloy are shown in Tables 3 and 4, respectively. Prior to the LSP treatment, the samples were polished mechanically with sand paper of different grades of roughness to achieve a mirror-like surface, which will enable the nano-indentation test requiring low surface roughness of several hundred nanometers. The polishing was followed by ultrasonic cleaning first with acetone and then deionized water to degrease the sample surface. All samples were prepared shortly before the LSP experiments.

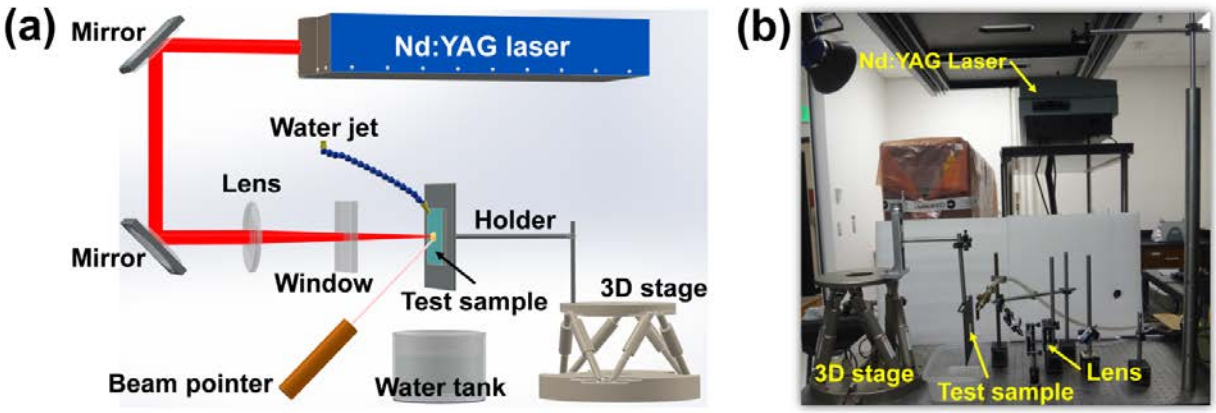

Fig. 2. (a) Schematic diagram of the experimental setup for LSP system. (b) LSP system established in LANE lab.

2.1.3 Experimental setup

Figure 2a shows the schematic diagram of the experimental setup for LSP system. The LSP system developed in our lab is shown in Fig. 2b. This LSP system can meet the demands of a single LSP impact and multiple LSP impacts. The laser source is a continuum Q-switched Nd:YAG PR II 8010 laser. The laser pulse frequency could be changed from 1 to 10 Hz. The normally used pulse duration of this laser is approximately 6-8 ns, and the maximum pulse energy is 650 mJ with a wavelength of 1064 nm. The output diameter of the laser beam from laser is about 5 mm. Two flat mirrors and a flat convergent lens (focal length: 20 cm) were used to deliver the pulse produced by the laser. The samples were vertically placed at the focal plane. The size of laser spot focused on the samples was measured to be approximately 1 mm. In this LSP system, the purified water was used as the confining medium. Control of water purity is important in order to avoid the formation of water bubbles or the concentration of impurities coming from the material ablation due to the laser irradiation. The appearance of suspended elements can affect the LSP process by their interaction with pulsed laser beam. Water in continuous condition is good solution to avoid these elements. Therefore, a special device to produce controlled water jets has been implemented to form a thin water layer on the sample surface to be treated. Taking care of the water velocity and jet direction, it is possible to produce a water layer with constant thickness. Aluminum (Al) foil tape and flat black tape have been chosen as the sacrificial layers. Before LSP experiment, the sample surfaces were covered with an Al foil or a layer of black tape with the thicknesses of 100 and 177 μm, respectively. The prepared sample was fixed on a holder and mounted on a motor controlled five-axis work stage with five degree of freedom and with resolution of 1 μm and maximum speed of 20 mm/s. The processing parameters of LSP are summarized in Table 5.

Table 5. The processing parameters used in LSP experiment

Laser system	Continuum Nd:YAG PR II 8010 laser; Wavelength: 800 nm; Pulse energy: 650 mJ; Pulse duration: 6-8 ns; Frequency: 1-10 Hz; Beam size: ~1 mm
Confining medium	Flowing water with layer thickness of approximately 1-2 mm
Sacrificial coating	(1) No coating; (2) Al foil tape (100μm); (2) flat black tape (177 μm)

Two different LSP experiments were designed during this reporting period. (1) Single spot LSP experiment: we used laser source with a frequency of 1 Hz for conveniently controlling the laser impact times on one point. (2) Large area LSP experiment: we used laser source with a frequency of 10 Hz for large area LSP by adjusting the overlap of laser spots. Figure 3 shows the schematic of laser processing on a sample in a large-scale area. The overlapping rate η in two directions is defined to describe and control the distribution of laser pulses on the impact region, which can be expressed as $\eta_L=(\Delta L/D)\times 100\%$, where ΔL is the coincidence length of overlapped two successive laser spots and D is the spot diameter, as shown in Fig. 3. Overlap of laser pulses was obtained by coupled computer control of velocity of continuous scanning in X-direction and step interval in the Y-direction. Every step along Y-direction is activated after a continuous movement in the X-direction with the required distance.

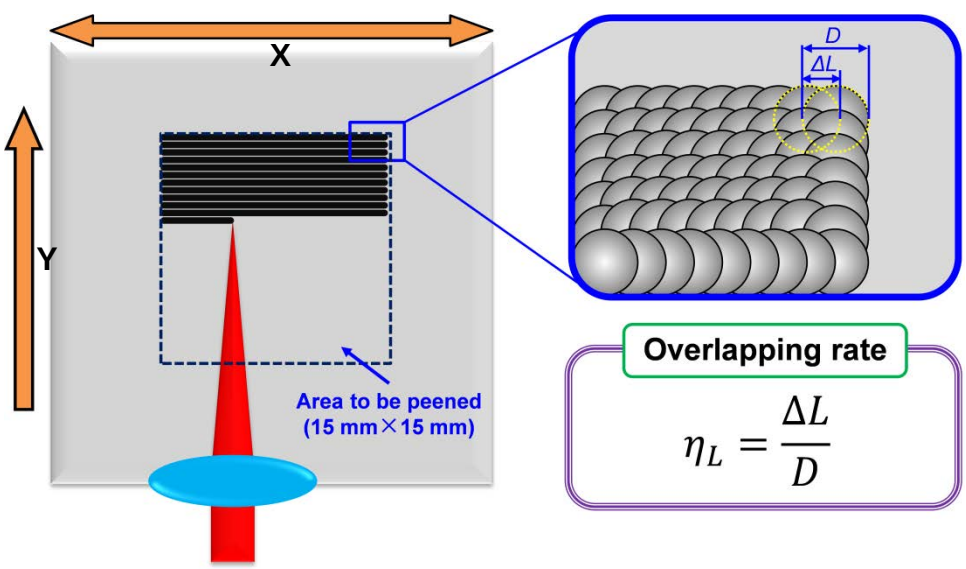

Fig. 3. Schematic of laser processing on a sample in a large scale area.

2.1.4 Characterization

After laser shock peening, the surface quality of the processed samples were systemically investigated. Various analytical techniques were used for characterization of the samples before

and after LSP for optimizing the LSP parameters. Optical microscopy (Nikon ECLIPSE, Japan) and electrical scanning microscopy (SEM, Philips, XL 30E, 5kV) were used to study the morphology of laser-peened samples. 3D profiler (New View 8000, Zygo Corporation) was used to measure the 3D profiles of the macro plastic deformation from the bottom surface of samples. A Raman spectrometer (Renishaw InVia plus, Renishaw, Gloucetershire, U.K.) with an excitation wavelength of 514 nm and a lateral resolution of approximately 1 μm was used to characterize the microstructure of the laser-peened samples. The micromechanical properties of all tested samples were carried out using nano-indentation (Hysitron nanoindenter) (Fig. 4a). All nanoindentation measurements were performed with the standard three-sided pyramidal Berkovich (TI-00039) probe. In all nanoindentation tests, a total of five indents were measured and averaged to determine the mean surface nano-hardness (*H*) and elastic modulus (*E*) values for statistical purposes. In the Al-Mg alloy nanoindentation experiment, the loading rate, maximum applied load, and loading time are 500 uN/s, 10000 uN, and 20/5/20 s, respectively (Fig. 4b); while in the SS nanoindentation experiment, the loading rate, maximum applied load, and loading time are 500 uN/s, 1500-5000 uN, and 10/5/10 s, respectively (Fig. 4c).

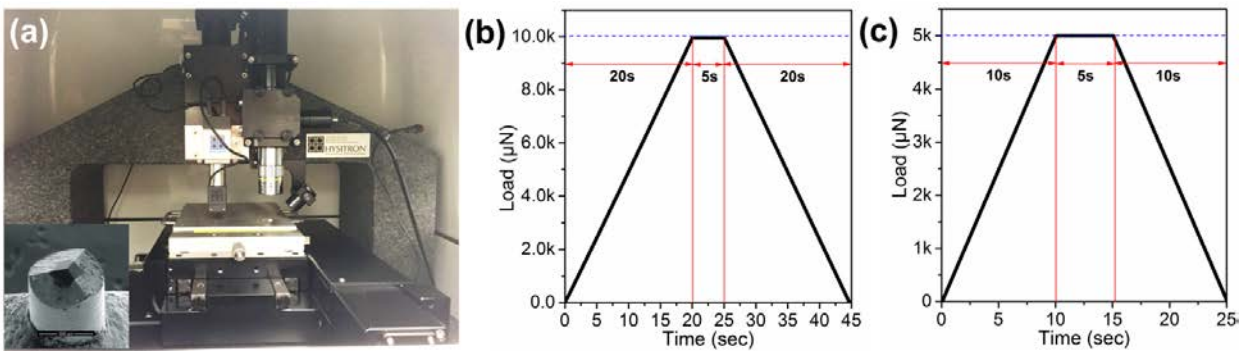

Fig. 4. (a) An optical image of nanoindenter used for mechanical property tests. The inset in (a) shows a typical SEM image of nanomechanical testing probe used in our experiment. (b,c) Load-time $F = F(t)$ function for time-dependent indentation in the experiments of LSP of (b) Al-Mg alloy, and (c) stainless steel.

2.2 Results and discussion

3.2.1 Optimization of the processing parameters of LSP using Al-Mg alloy

The important processing parameters related to LSP conditions are laser processing parameter, confining medium, and sacrificial coatings, which can significantly affect the mechanical properties of the alloy and metallic materials. The objective of this part is to investigate the effect of LSP in metal components using Al-Mg alloy as the tested samples.

3.2.1.1 The effect of sacrificial coatings on LSP

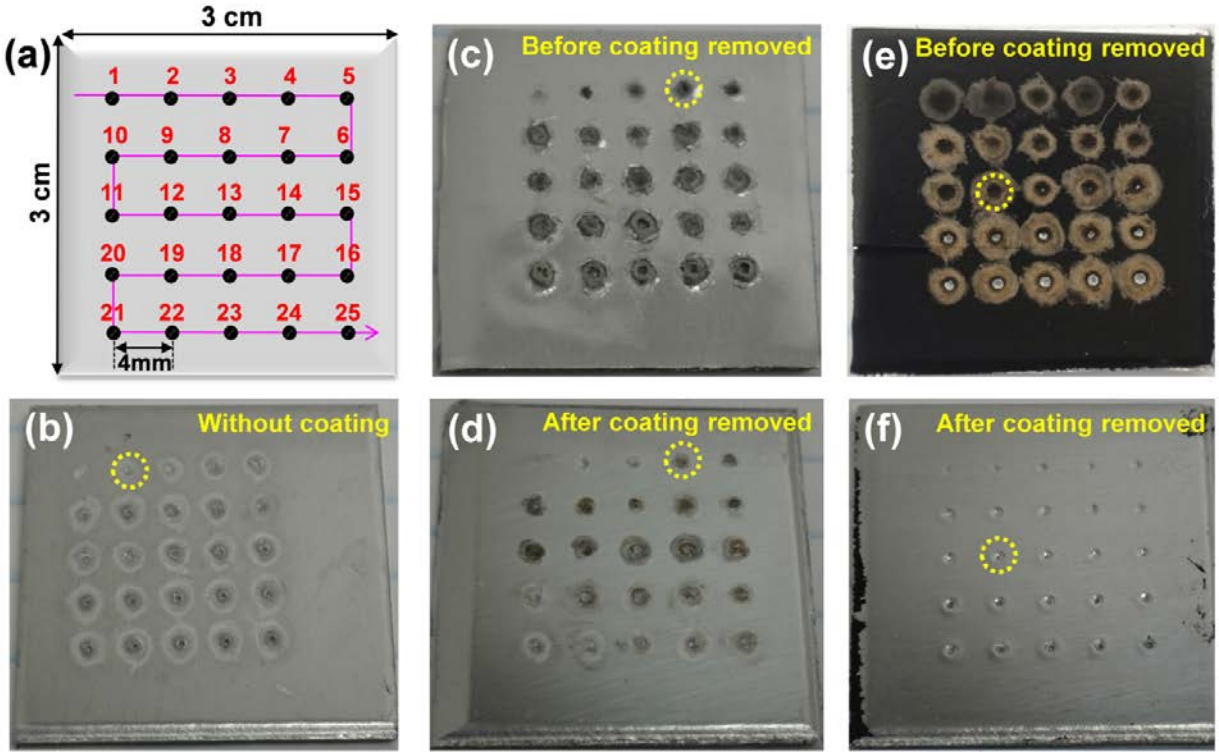

Fig. 5. (a) Schematic of the point distribution with different LSP impacts. (b-f) Laser-peened Al-Mg alloy samples (b) without sacrificial coating, using (c,d) Al foil tape and (e,f) black tape as the sacrificial coatings.

The use of absorbent sacrificial coatings is found to increase the shock wave intensity in addition to the protection of the sample's surface from laser ablation and melting. Therefore, it is very important to select the effective and practical sacrificial coatings for LSP applications. In Fig 5a, the schematic of LSP-impacted points on Al-Mg alloy samples with different impact times from 1 to 25 is shown. The distance between nearby impacted points is about 4 mm, which could avoid the interactions among different points. Figures 5b to 5f show the optical images of laser-peened Al-Mg alloy sample plate (b) without sacrificial coating, using (c,d) Al foil tape, and black tape as the sacrificial coatings, respectively. Obviously, increasing LSP impact times could result in higher possibility of laser damage to the sample surfaces. The dashed yellow circles used in Figs. 5b to 5f indicate the impacted points from which the penetration of the sacrificial coating or alloy surface damage could be observed. In Fig. 5b, laser-peened sample plate without any sacrificial coating shows surface damage from 2 LSP impacts. Figures 5c and 5d show the laser-peened sample with Al foil as sacrificial coating (c) before and (d) after coating removed, respectively. The penetration of the coating in Fig. 5c and the damage of alloy surface in Fig. 5d both begin from 4 LSP impacts. The laser-peened samples with black tape as sacrificial coating before and after coating removed are shown in Fig 5e and 5f, respectively. However, under this

condition, the penetration of coating and the damage of alloy surface start from 12 LSP impacts, which is much higher than that with Al foil. Apparently, the black tape could endure more laser impacts than Al foil, while it is easier for the LSP without sacrificial coating to damage the sample surfaces. The surface damage induced by laser direct irradiation should be avoided during the LSP process, which could increase the surface roughness, decrease the residual stress and reduce the corrosion resistance. On the other hand, higher impact times are preferred to generate higher residual stress and better corrosion resistance. Thus, the black tape is considered to be the prior sacrificial material and will be used in the following experiments.

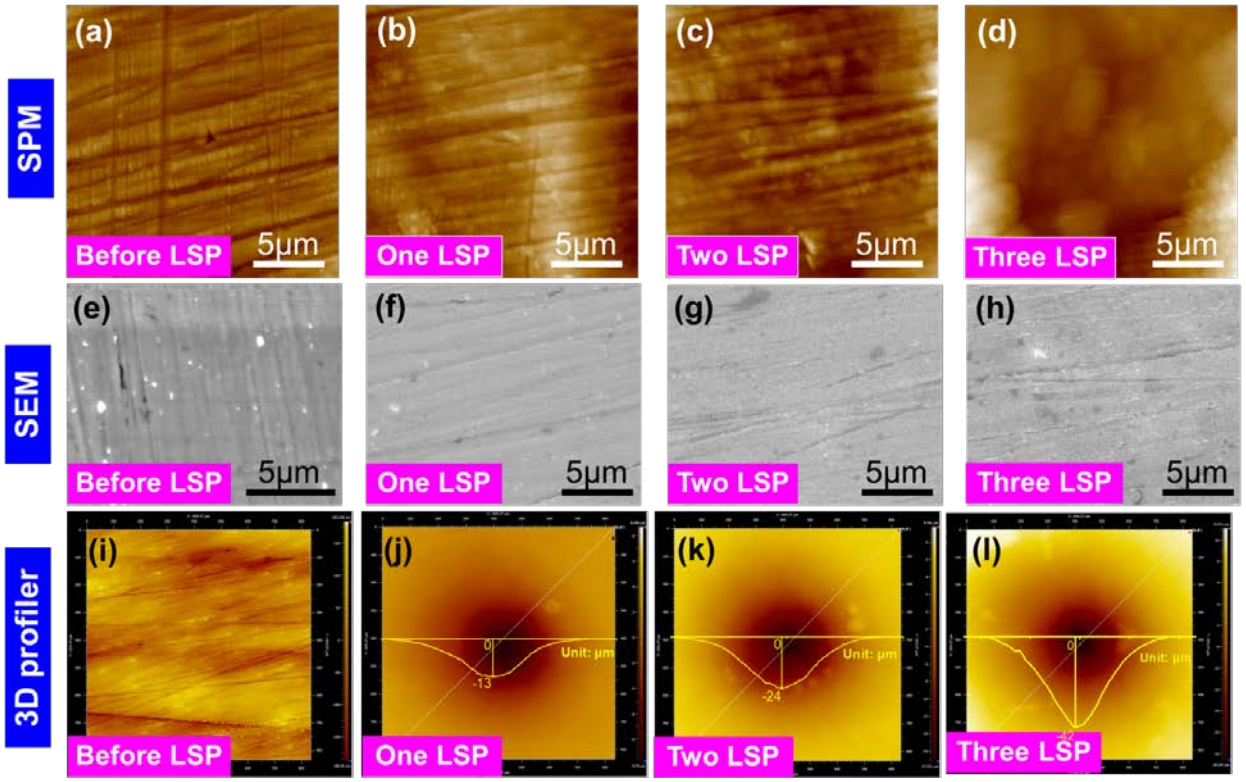

Fig. 6. (a-d) SPM images of the Al-Mg alloy surfaces treated by single pulse LSP for (a) 0, (b) 1, (c) 2 and (d) 3 impacts. Corresponding (e-h) enlarged SEM images and (i-h) 3D surface topographies of the Al-Mg alloy shown in (a-d). Insets in (j, k, l) show the cross-sectional height profiles along the lines in the same images.

3.2.1.2 The effect of LSP impact time on the properties of Al-Mg alloy

A. Surface roughness and surface profile

SPM, SEM, and 3D profiler were used to characterize the surface roughness and profile variation of Al-Mg alloy due to laser shock peeing. As shown in Fig. 6, SPM (6a-6d) and SEM (6e-6h) images indicate that the surface roughness increase a little with LSP impact times increasing, which is inevitable for LSP process and will not affect the residual stress and corrosion resistance seriously. On the other hand, the 3D surface topographies (6i-6l) reveal that the depth

of the laser-peened area (dents) increase proportionally with higher impact times. With one, two, and LSP impacts, the dent depths are 13, 24, and 42 μm, respectively. This result indirectly indicates higher hardness and residual stress of the dents with increasing the impact times.

B. The effect of LSP on surface nano-hardness and elastic modulus

Nanoindentation has been established as a powerful technique to characterize the mechanical properties at small scales. The force required to press a sharp diamond indenter to the tested samples is recorded as a function of indentation depth. Both elastic modulus and nano-hardness can be extracted directly from the nanoindentation curve. Elastic modulus and nano-hardness are determined based on the knowledge of the tip shape function, and the load-displacement curve (load F and displacement H).[4] Figure 7d shows the typical load-displacement curve of Al-Mg alloy without LSP.

The nano-hardness H and elastic modulus E_r were defined as follows:

$$\mathrm{H} = \frac{P_{max}}{A} \tag{3.1}$$

$$E_r = \frac{\sqrt{\pi}}{2\beta}\frac{S}{\sqrt{A}} \tag{3.2}$$

where P_{max} is the maximum load, A is the projected contact area, S is the banner slope of the unloading curve and β is the contact compliance between the indenter and the sample, which is equal to the tangent to the force-displacement curve during unloading after correction for frame compliance. The symbol A in the above equations is calculated as:

$$\mathrm{A} = 24.56h_c^2 + \sum_{i=0}^{7} C\beta h_c^{1/2^i} \tag{3.3}$$

$$h_c = h - \beta P_{max}/S \tag{3.4}$$

where h_c is the contact depth and h is the indentation depth.

Figures 7a-c show the representative in-situ SPM images of Al-Mg alloy surfaces (a) before and (b,c) after nanoindentation, where obvious residual indentations are formed after nanoindentation, indicating residual indent impression. Figures 7d-f show the measured load-displacement curves of the Al-Mg alloy at a maximum load of 10000 μN treated by single pulse laser peening for (d) 0, (e) 1, and (f) 2 impacts, respectively. For each condition, the measurements were repeated five times, and an average value was determined on the basis of the five measured data. The corresponding calculated experimental data (surface nano-hardness, elastic modulus, contact depth) are shown in Fig. 8. From Fig. 8a, it can be found that the contact depths of the indenter are 602±13, 527±13, and (369±7) nm in the regions by LSP for 0, 1 and 2 impacts, respectively.

The maximum contact depths of the indenter decease rapidly from non-laser-peened region to laser-peened region, and further decrease with the increase of laser impact times (Fig. 8a).

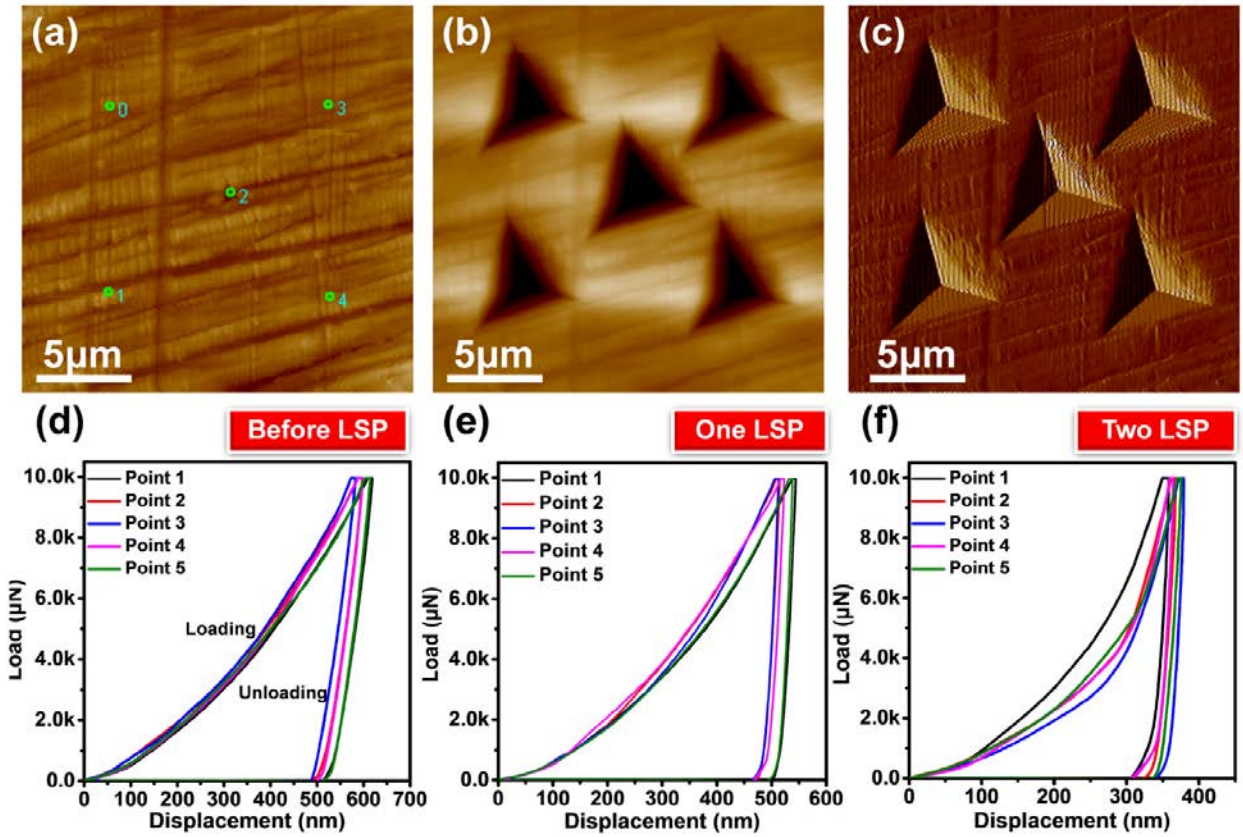

Fig. 7. (a) Representative SPM image of Al-Mg alloy surfaces before nanoindentation. (b,c) Corresponding and in-situ SPM (b) morphological and (c) phase images of the Al-Mg alloy after nanoindentation. (d-f) The measured load-displacement curves of the Al-Mg alloy treated by single pulse LSP for (d) 0, (e) 1, and (f) 2 impacts.

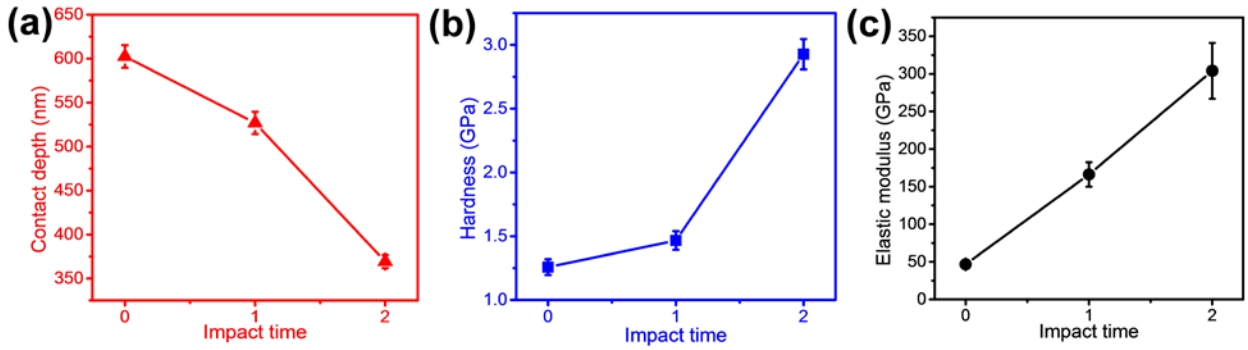

Fig. 8. The profiles of the (a) contact depth, (b) surface nano-hardness, and (c) elastic modulus of the Al-Mg alloy as a function of LSP impacts.

The measured value of surface nano-hardness for different laser impacts is shown in Fig 8b. It can be seen that the value of surface nano-hardness in the laser-peened region is improved obviously in comparison with the corresponding value in the non-laser-peened region. Surface

nano-hardness reaches about 1.47 GPa in the laser-peened region with singe impact time, which is larger by 15.9% than that in the non-laser-peened region (1.26 GPa). When the laser impact is increased to twice on one spot, the surface nano-hardness value reaches 2.93 GPa which is larger by 133% than in the non-laser-peened region. The dependence of elastic modulus on LSP impacts is shown in Fig. 8c. The value of elastic modulus is 47.7 GPa in the non-laser-peened region, and the corresponding value in the regions with single and two LSP impacts are 166.3 and 304.0 GPa, respectively. Namely, the value of elastic modulus in the regions with single and two LSP impacts are increased by 249% and 537% compared to that in the non-laser-peened region, respectively. The above analysis indicates that both the values of surface nano-hardness and elastic modulus in the laser-peened region are obviously larger than those in the non-laser-peened region, and increase with increasing of LSP impacts. Although the elastic modulus is an intrinsic property of the material and fundamentally relates to the atomic bonding, the elastic modulus can be changed by some surface treatment technologies. [5] It is well known that the increasing of elastic modulus is advantageous in enhancing stiffness of the samples, which decides the stability when the components service in environment. [6] Therefore, it can be concluded that LSP can improve the stiffness of the Al-Mg alloy. The enhancement mechanism of LSP on nano-hardness and elastic modulus will be investigated in the next reporting period.

3.2.1.3 Large area LSP

In order to realize industrial application, the ability of large area processing is necessary. Thus, the large area LSP experiments were implemented on the Al-Mg alloy samples with different overlapping rates. As shown in Figs. 9 a-d, LSP with different overlapping rates (0%, 25%, 50%, and 75%) were carried out and corresponding optical photos (e-h), SEM image (i-l) and 3D topographical images (m-p) are provided. According to the optical photos, the LSP induced dents become smaller when the overlapping rate increases from 0% to 50%, which is due to the decrease of distance between LSP points, while with 75% overlapping rate, the sample surface is seriously damaged due to the destroy of sacrificial coating by laser pulses. It can be seen from 3D profile images that, different from 0% (Fig. 9m) and 25% (Fig. 9n), with overlapping rate of 50% (Fig. 9o) no regular or obvious dent patterns could be found on the relatively flat surface, which might due to the multi-direction forces on the overlapping area from different LSP impact points. On the other hand, the inserted cross section height profiles below the 3D topographical images of Figs. 9m-p exhibit almost unchanged surface roughness with 0%, 25%, and 50% overlapping rates, and a sharp increase with 75% overlapping rate which indicates the damage of the sample surface. The unchanged roughness and relatively flat surface under the condition of 50% overlapping rate could be explained by the SEM images (Fig. 9i-l). As is shown in the SEM images, some small irregular wrinkle could be observed for 25% (Fig. 9j) and 50% (Fig. 9k) overlapping rates, which would definitely increase localized surface roughness. These wrinkles could also be recognized in the 3D profile images (Figs. 9n and 9o) as those of small protrude

points. Therefore, the increased overlap (0% to 50%) could obscure the dents and generally flatten the sample surface as well as increase the localized surface roughness, resulting in unchanged surface roughness in total. Take these results into consideration, 50% overlapping is the most favorable rate for large area LSP on Al-Mg alloy.

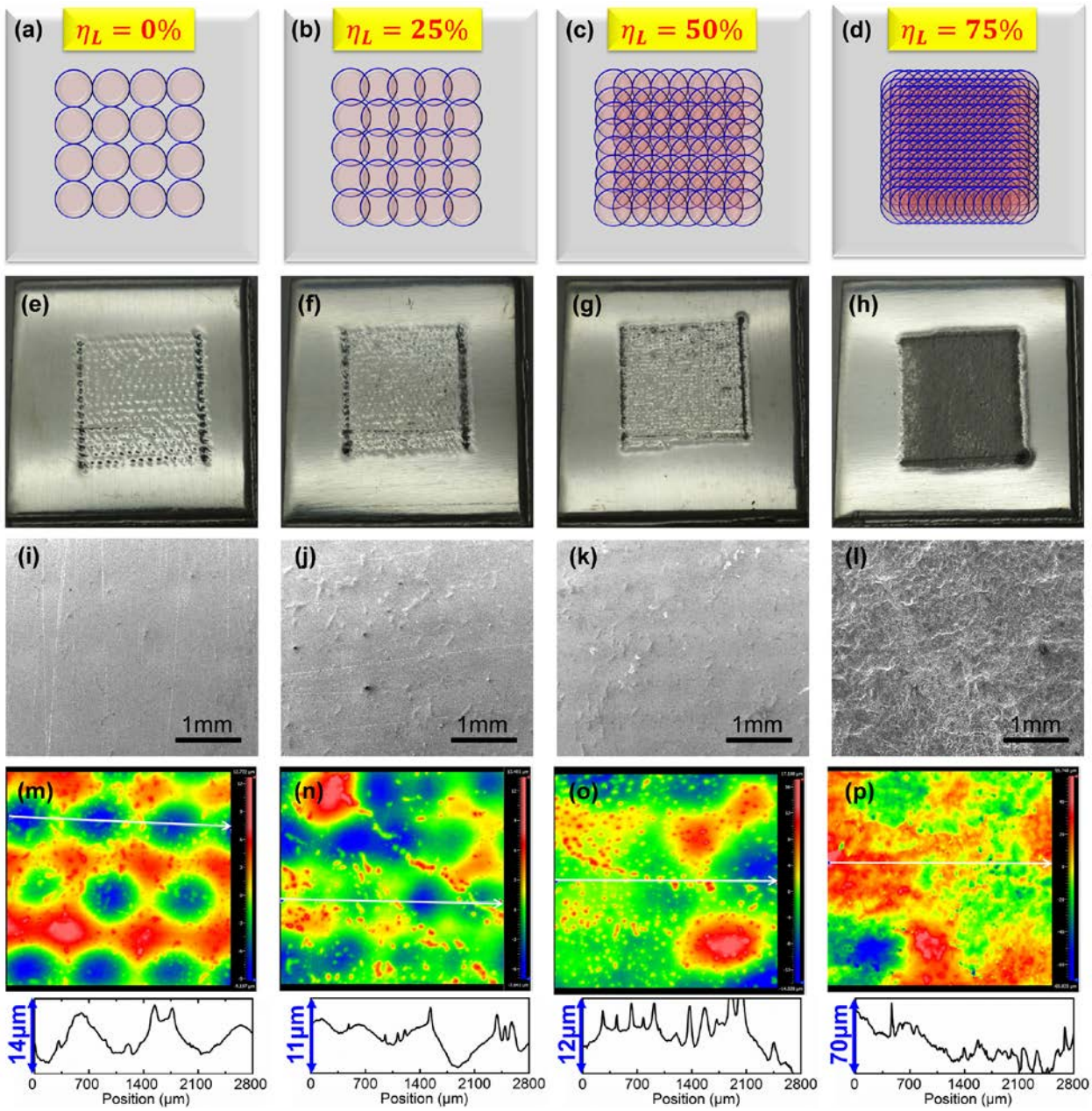

Fig. 9. The schematic of shocking path by LSP with different overlapping rates η_L of (a) 0%, (b) 25%, (c) 50% and (d) 75%. The corresponding (e-h) optical, (i-l) SEM, and (m-p) 3D surface topographical images of the sample plates after LSP with different overlapping rates shown in (a-d). Insets in (m-p) show the cross-sectional height profiles along the lines in the same images.

3.2.2 Analyses of laser-peened 310 SS

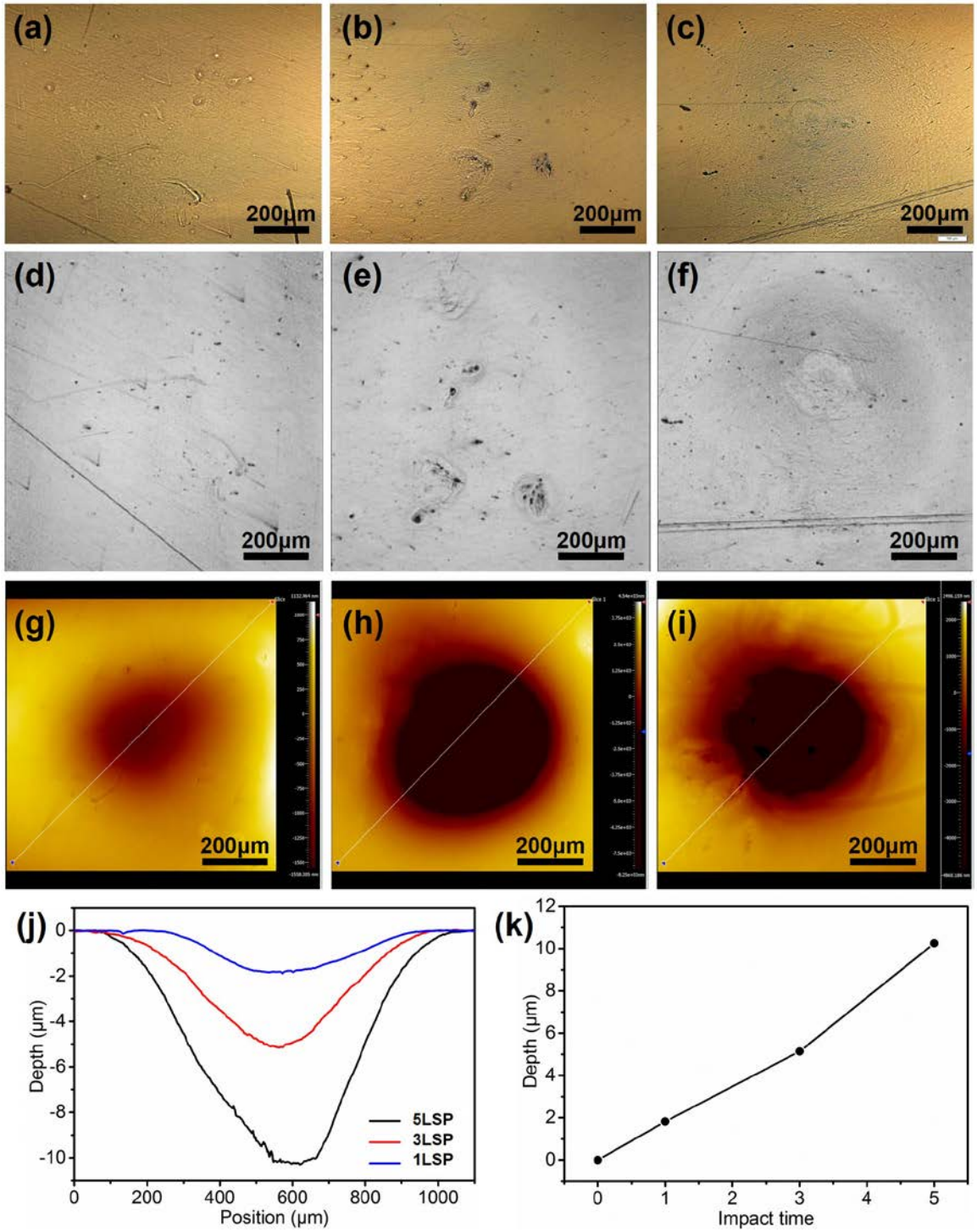

Fig. 10. (a-d) Optical micrographs of 310 SS sample surfaces treated by single pulse LSP for (a) 1, (b) 3, and (d) 5 impacts. Corresponding (d-f) SEM images and (g-i) 3D surface topographies of the 310 SS surfaces shown in (a-d). (j) Dent depths with different LSP impacts. (k) The depth of dent center as a function of LSP impacts.

A. Surface roughness and surface profile

310 stainless steel, one commonly used steel alloy, was selected for the single point LSP experiments. Figure 10 shows the influence of the LSP impact times on the surface roughness and morphology of 310 SS sample plate. From the optical micrographs (Fig. 10a-c) and SEM images (Fig. 10d-f), small dents and defects are observed to increase when LSP impacts arise from 1 to 5, indicating the increase of the localized surface roughness. Figures 10g-i show the corresponding 3D surface profiles of the dents formed by LSP for 1, 3 and 5 impacts. It can be concluded from the cross-sectional profile in Fig. 10j that the dent depths increase with the LSP impact times. Figure 10k shows the depth of dent center as a function of LSP impacts that the dent depth increases nearly proportionally to the LSP impacts. With 1, 3, 5 LSP impacts, the dent depths are 2 μm, 5μm, and 10μm, respectively. This trend is the same as the LPS impact results with Al-Mg alloy.

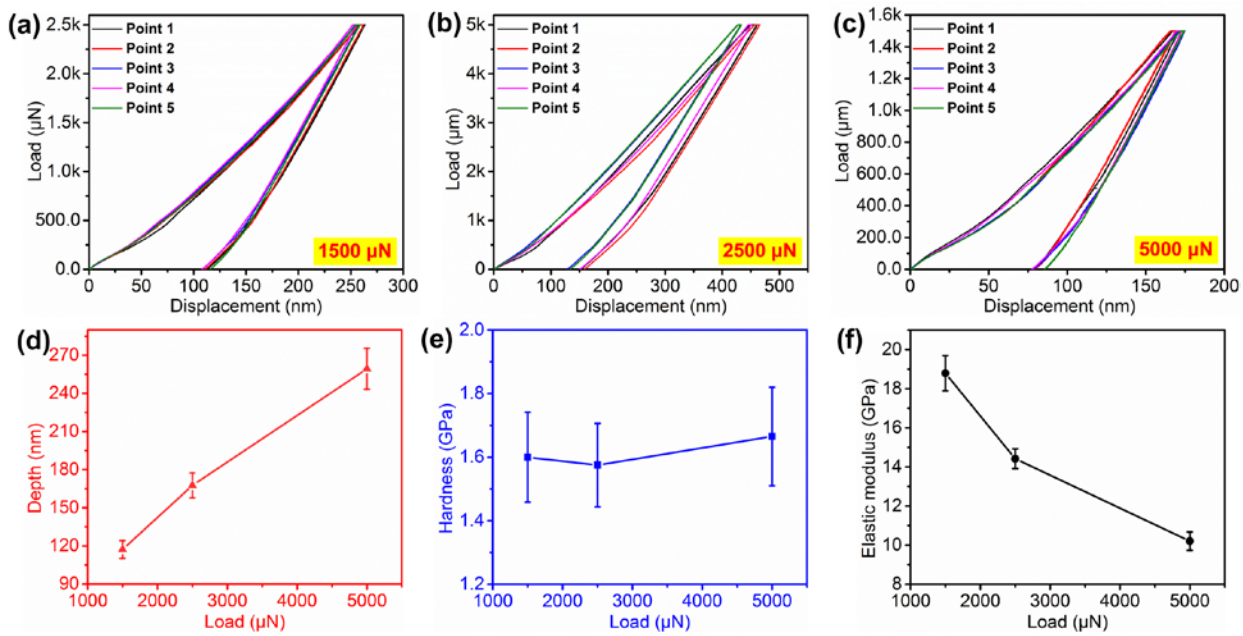

Fig. 11. The measured load-displacement curves for the 310 SS samples with a single LSP impact at different maximum loads of (a) 1500 μN, (b) 2500 μN, and (c) 5000 μN. The profiles of the (d) contact depth, (e) surface nano-hardness, and (f) elastic modulus of the 310 SS samples as a function of the maximum load.

B. The effect of LSP on nano-hardness and elastic modulus

Firstly, the elastic modulus and nano-hardness distribution of the 310 SS sample under different maximum loads are investigated. Figures 11a-c show the measured load-displacement curves for the 310 SS sample with a single LSP impact at different maximum loads of (a) 1500 μN, (b) 2500 μN, and (c) 5000 μN, respectively. It can be found that the contact depths of the indenter of the 310 SS samples with a single LSP impact are 117.2 nm, 167.6 nm, and 259.4 nm at different

maximum loads of 1500 μN, 2500 μN, and 5000 μN, respectively. It is clearly observed that the maximum contact depth increases with increasing of the maximum load (Fig. 11d). Figures 11e and 11f show the profiles of the (e) surface nanohardness, and (f) elastic modulus of the 310 SS samples as a function of the maximum load with 1500 μN, 2500 μN, and 5000 μN. The value of elastic modulus of the 310 SS samples decreases with the increase of the maximum load. However, there is no obvious change for the surface nano-hardness with the increase of the maximum load from 1500 μN to 5000 μN, this phenomenon may be explained by that fact that, though the contact depth of the indenter increases with increasing of the maximum load, the nano-mechanical property keeps unchanged until reaching up to a certain depth to the treated surface.

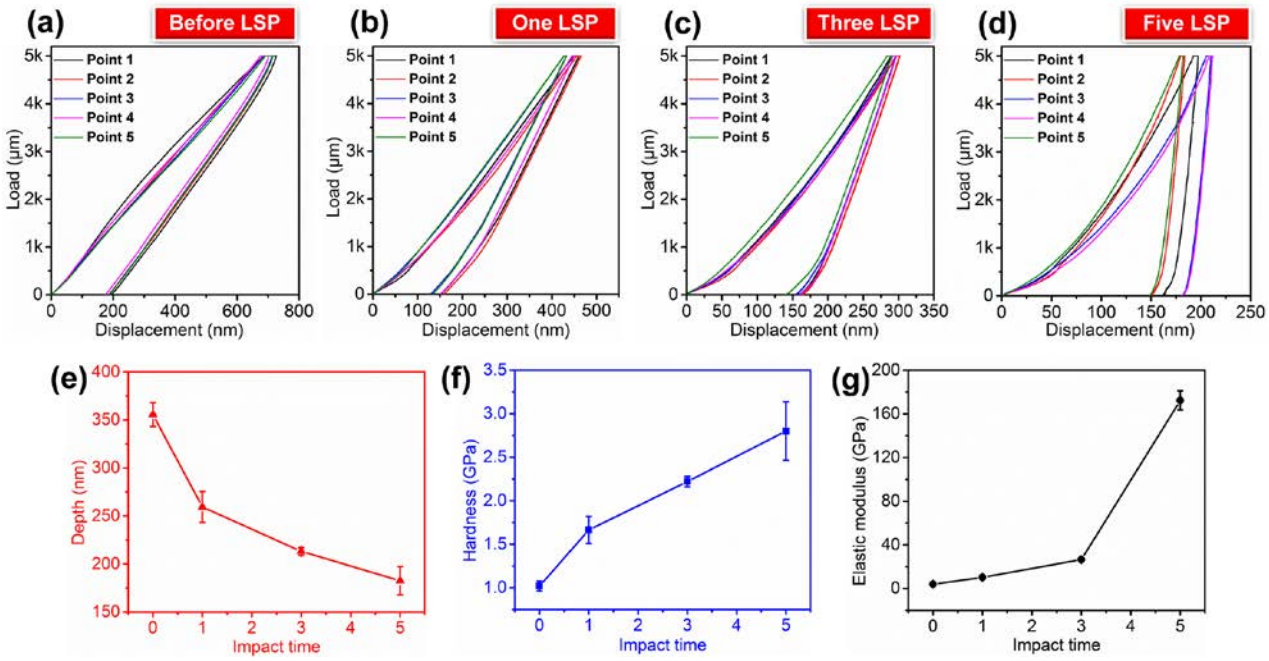

Fig. 12. The measured load-displacement curves of the 310 SS samples treated by single pulse LSP for (a) 0, (b) 1, (c) 3, and (d) 5 impacts. The profiles of the (e) contact depth, (f) surface nano-hardness, and (g) elastic modulus of the 310 SS samples as a function of LSP impacts.

Figures 12a-d show the measured load-displacement curves of the 310 SS samples at maximum load of 5000 μN and treated by single spot LSP for (a) 0, (b) 1, (c) 3, and (d) 5 impacts. It is found that the contact depths of the 310 SS samples are 355.6, 259.4, 213.1, and 182.7 nm after LSP for 0, 1, 3, 5 impacts, respectively. The maximum contact depth is observed to decrease with the increase of LSP impacts. From Figs. 12a-d, the values of surface nano-hardness and elastic modulus of the samples before and after LSP with different impacts are shown in details. The values of nano-hardness are 1.0 GPa, 1.7 GPa, 2.2 GPa, and 2.8 GPa after LSP for 0, 1, 3, 5 impacts, respectively. The values of elastic modulus are 4.0 GPa, 10.2 GPa, 26.5 GPa, and 172.4 GPa after LSP for 0, 1, 3, 5 impacts, respectively. Figures 12e and 12f exhibit the profiles of the (e) surface nano-hardness, (f) elastic modulus of the 310 SS samples as

a function of LSP impacts. Similar to the Al-Mg alloy, the values of the surface nano-hardness and elastic modulus for the laser-peened samples are obviously larger than those of non-laser-peened samples. In addition, the values of surface nano-hardness and elastic modulus of the sample increase with the increase of the LSP impacts. The values of surface nano-hardness are increased by 70%, 120%, and 180% than that in the non-laser-peened region when the number of laser impacts increases from 1 to 3 and then to 5, respectively; while the values of elastic modulus are increased by 155%, 563%, and 4210%. Therefore, it can be concluded that single and multiple LSP impacts can improve the nano-hardness and elastic modulus, which is favorable in enhancing the stiffness and the possible corrosion resistance of the stainless steel.

3.2.3 Analysis of the laser-peened 304 SS

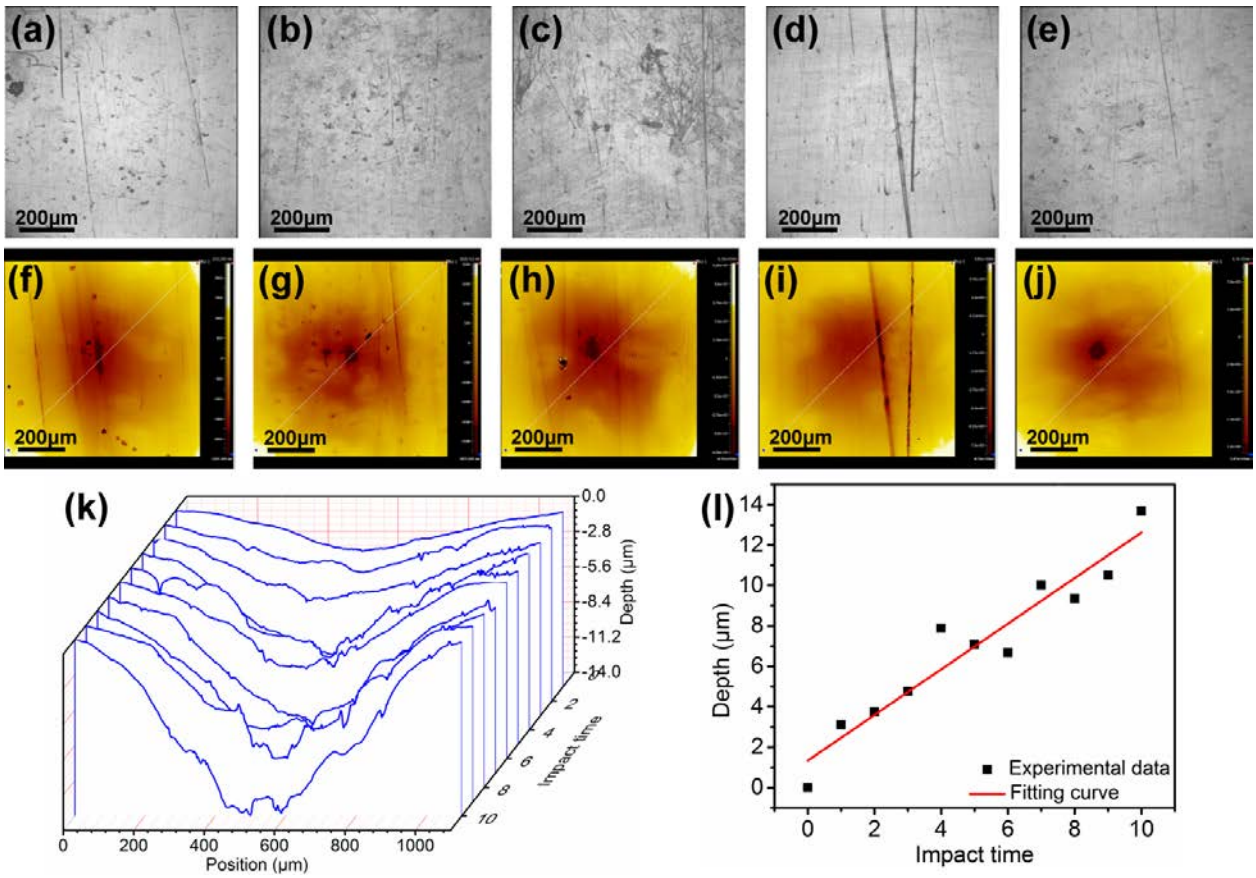

Fig. 13. (a-e) SEM images and (f-j) corresponding 3D surface topographies of the 304 SS sample surfaces by single pulse laser shock peening for (a) 1, (b) 2, (c) 4, (d) 7, and (e) 10 impacts. (k) Dent depths with different laser pulse impacts. (l) The depth of dent center as a function of LSP impacts.

A. Surface roughness and surface profile

304 stainless steel is one of the most popular pipeline materials due to its high strength and high corrosion resistance. For single point LSP experiment, the influence of LSP impact times on surface roughness and morphology of the 304 SS sample plate was investigated and is shown in

Fig 13. It is observed from the SEM images (Fig 13a-e) that the small dents and defects increase generally as LSP impacts arise from 1 to 10, indicating the increase of the localized surface roughness. Figures 13f-j exhibit the corresponding 3D surface profiles of the dents with 1, 2, 4, 7, and 10 LSP impacts, and the cross-sectional profile is shown in Fig. 13k. The dent depth is observed to increase with the LSP impact times. Figure 13l shows the depth of dent center as a function of LSP impacts. The depth of the dent center increases nearly proportionally to the LSP impact times and a linear fitting curve could be made with acceptable standard deviation. This trend confirms the similar LPS impact results with Al-Mg alloy and 310 SS.

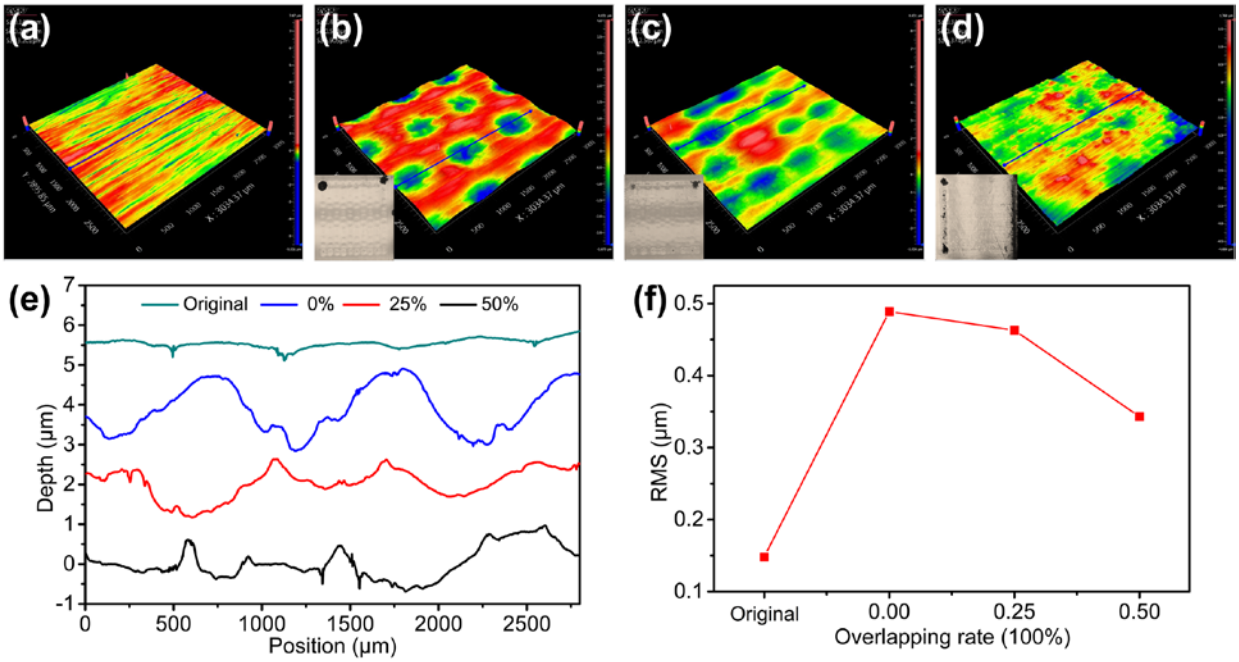

Fig. 14. 3D surface topographies of the 304 SS sample surfaces (a) before LSP and (b-d) after LSP with different overlapping rates of (b) 0%, (c) 25%, and (d) 50%. Insets in (b-d) show the corresponding optical images of the samples in the same images. (e) Surface deformation of the same sample along the line in the corresponding images. (f) Comparison of surface roughness with different overlapping rates.

B. Large-area LSP

For future industrial application, large area LSP experiments were also implemented on 304SS with different overlapping rates. As shown in Fig. 14, LSP with different overlapping rates were carried out and corresponding 3D topographical images as well as the optical photos (a-d) are provided. Fig. 14a show the sample surface without any LSP process, which is the most flat, followed with the samples after LSP (Figs. 14b-d) with 0%, 25%, and 50% overlapping rates, respectively. LSP with 75% overlap will seriously damage the sample surface and thus ignored. As we can see, the LSP induced dents become smaller when the overlapping rate increases from 0% to 25%, which is due to the decrease of distance between LSP points. Different from 0% (Fig.

14bm) and 25% (Fig 14c), with overlapping rate of 50% (Fig 14d), no regular or obvious dent patterns could be found on the relatively flat surface. The cross-sectional view of the dents with overlapping rates (Fig. 14e) show the abrupt dent generation from original sample to laser-peened sample with 0% overlap, as well as the gradually flattened surface with the overlapping rate increasing from 0% to 50%. Though some small protrude points is observed in Fig 14d, similar with the phenomenon on the laser-peened Al-Mg alloy samples, the surface roughness still decrease as overlapping rates increase from 0% to 50%, as is shown in Fig. 14f. In conclusion, 50% overlap is the most favorable for large area LSP on 304 SS.

Key outcomes

In the first reporting period of this project, the experimental setup for laser shock peening system has been completely developed in our lab. The effects of LSP on the surface morphology, nano-hardness, and elastic modulus of the tested sample (Al-Mg alloy, 310 SS, 304 SS) have also systemically investigated and analyzed. Some important conclusions have been summarized as follows:

(1) The experimental setup for LSP system has been successfully developed. This LSP system can meet the demands of a single LSP impact and multiple LSP impacts. The laser source is a continuum Q-switched Nd:YAG PR II 8010 laser. The laser pulse frequency could be changed from 1 to 10 Hz. The normally used pulse duration of this laser is approximately 6-8 ns, and the maximum pulse energy is 800 mJ with a wavelength of 1064 nm. The output diameter of the laser beam from laser is about 5 mm. Two flat Nd:YAG mirrors and a flat convergent lens (focal length: 20 cm) were used to deliver the pulse produced by the laser. A flowing water film with a layer thickness of 1-2 mm was used as a transparent confining medium. The black tape with a thickness of 177 μm was optimized as sacrificial layer to protect the sample surface from the thermal effect.

(2) With appropriate processing parameters, macro plastic deformations (dents) can be formed on the sample surfaces through ns laser-induced shock waves. Surface morphologies and 3D profiles of dents have been measured. Both surface roughness and dent depth are increased with increasing of the LSP impact times.

(3) For all tested samples (A-Mg alloy, 310 SS, 304 SS), the contact depths for the laser-peened samples are lower than those for the non-laser-peened samples; the values of surface nano-hardness and elastic modulus for the laser-peened samples are obviously larger than those for the non-laser-peened samples. In addition, the values of surface nano-hardness and elastic modulus are increased with increasing of LSP impact times. The improvement of the surface nano-hardness and elastic modulus is considered to be favorable for improving the stiffness and corrosion resistance of these components used for pipeline construction.

(4) The effect of overlapping rate on large area LSP has been investigated. An approximate overlapping rate is beneficial to obtain a relatively smooth surface and a possible homogeneous residual stress field (need to be verified in the next reporting period). 50% overlapping rate can be selected for the LSP treatment of Al-Mg alloy and stainless steel samples due to the LSP effect and the work efficiency.

(c) Description of any Problems/Challenges

No problem was experienced during this reporting period.

(d) Planned Activities for the Next Quarter

The specifically planned objectives and activities to be accomplished during the next period (January 1, 2015 to March 31, 2015) are listed as follows.

Table 5. The planned objectives and activities for the second quarter

Objectives	Activities
(a) Surface evaluation of laser-peened samples	1) To study the depth profile of the nano-hardness/elastic distribution the laser-peened sample using nanoindenation technique; 2) To conduct the depth profile compressive residual stress measurement the laser-peened sample using X-ray diffraction $\sin^2\Psi$ method; 3) To investigate the grain refinement mechanism of LSP impacts stainless steel by means of cross-sectional optical microscopy a transmission electron microscopy observation;
(b) The corrosion resistance test of laser-peened sample surfaces	1) Sample preparation for the corrosion test; 2) Selection and preparation of corrosion solution. 3) Corrosion test and analysis of the laser-peened samples.
(c) Further optimization of processing parameters for LSP	1) Processing of SS samples with different LSP impacts and laser energy; 2) Surface evaluation (XRD, nanoindenation, TEM, corrosion tests) these laser-peened samples to obtain optimized LSP impacts and la energy; 3) Repetition of procedures (a) and (b) to obtain the LSP parameters wh could induce high compressive residual stress and corrosion resistance

References

[1] Fairand, B. P.; Clauer, A. H., Effect of water and paint coatings on the magnitude of laser-generated shocks. *Optics Communications* **1976,** *18* (4), 588-591.

[2] Fairand, B. P.; Wilcox, B. A.; Gallagher, W. J.; Williams, D. N., Laser shock - induced microstructural and mechanical property changes in 7075 aluminum. *Journal of Applied Physics* **1972,** *43* (9), 3893-3895.

[3] Caslaru, R.; Guo, Y.; Sealy, M.; Chen, S., Fabrication and characterization of micro dent array produced by laser shock peening on aluminum surfaces. *Trans. NAMRI/SME* **2009,** *37*, 159-166.

[4] Doerner, M. F.; Nix, W. D., A method for interpreting the data from depth-sensing indentation instruments. *Journal of Materials Research* **1986,** *1* (04), 601-609.

[5] Zhang, Y. K.; Zhang, X. R.; Wang, X. D.; Zhang, S. Y.; Gao, C. Y.; Zhou, J. Z.; Yang, J. C.; Cai, L., Elastic properties modification in aluminum alloy induced by laser-shock processing. *Materials Science and Engineering: A* **2001,** *297* (1–2), 138-143.

[6] San, J.; Wang, Z.; Li, S.; Liu, J., Nano-hardness and wear properties of C-implanted Nylon 6. *Surface and Coatings Technology* **2006,** *200* (18–19), 5245-5252.